

Persistence of Topological Phases in Non-Hermitian Quantum Walks

Vikash Mittal,¹ Aswathy Raj,² Sanjib Dey,^{1,*} and Sandeep K. Goyal^{1,†}

¹*Department of Physical Sciences, Indian Institute of Science Education & Research (IISER) Mohali,
Sector 81 SAS Nagar, Manauli PO 140306 Punjab, India*

²*Department of Physics, Indian Institute of Science Education & Research (IISER) Bhopal,
Bhopal Bypass Road, Bhauri, Bhopal 462066, India*

Discrete-time quantum walks are known to exhibit exotic topological states and phases. Physical realization of quantum walks in a noisy environment may destroy these phases. We investigate the behavior of topological states in quantum walks in the presence of a lossy environment. The environmental effects in the quantum walk dynamics are addressed using the non-Hermitian Hamiltonian approach. We show that the topological phases of the quantum walks are robust against moderate losses. The topological order in one-dimensional split-step quantum walk persists as long as the Hamiltonian is \mathcal{PT} -symmetric. Although the topological nature persists in two-dimensional quantum walks as well, the \mathcal{PT} -symmetry has no role to play there. Furthermore, we observe the noise-induced topological phase transition in two-dimensional quantum walks.

I. INTRODUCTION

Quantum walks are the quantum analog of classical random walks [1–5] where a quantum walker propagates on a lattice and the direction of propagation is conditioned over the state of its coin. Due to the quantum nature of the walker and the coin, the position state of the walker is a superposition of multiple lattice sites. This provides a quadratically fast spread of the walker over the lattice as compared to its classical counterpart [2]. Quantum walks, continuous-time as well as discrete-time, are important in various fields including universal quantum computation [6–8], quantum search algorithms [9–12], quantum simulations [13], quantum state transfer [14] and simulation of physical systems [15–17]. Quantum walks have been used in other branches of science as well, such as in biology to study the energy transfer in photosynthesis [18]. They have also been proved as a promising candidate to simulate the decoherence [19, 20] and to implement generalized measurements (POVM) [21].

Quantum walks have started gaining popularity among condensed matter physicists since the last decade because one can simulate exotic topological phases using one (1D) and two-dimensional (2D) discrete-time quantum walk (DTQW) [22–25]. As a consequence, people have been able to establish the bulk-boundary correspondence for 1D periodic systems [26, 27]. These versatilities of quantum walks make them a prime candidate for fault-tolerant topological quantum computation and quantum simulations.

Quantum walks have been implemented on a variety of systems, such as; trapped ions/atoms [28–31], optical systems [32–37], NMR [38, 39], Bose-Einstein condensate [40], etc. However, no quantum system is without losses, due to which implementation of quantum algorithms as

well as the observation of exotic topological phases have always been difficult. In this article, we study the effect of losses on the topological phases arising in quantum walk systems. A system along with losses effectively renders the quantum walk dynamics non-unitary. We treat this non-unitary evolution using the non-Hermitian Hamiltonian approach [41, 42]. We establish that for a 1D split-step quantum walk (SSQW), the topological phases persist as long as the spectrum of the non-Hermitian Hamiltonian is real. In other words, as long as the underlying non-Hermitian Hamiltonian is \mathcal{PT} -symmetric [41], the topological phase is preserved.

2D quantum walks have a more complex structure. In this case, too, we observe the persistence of the topological phases. However, \mathcal{PT} symmetry is absent in 2D DTQW upon introducing the noise. This is because quasi-energies in the case of two dimensional are complex even for a very small value of the scaling factor. Furthermore, noise-induced phase transition can be observed in these 2D DTQWs.

Non-Hermitian quantum walk has been studied theoretically [43] as well as experimentally [34]. The existence of topological edge states [44], topological transition [45–47] as well as the correspondence between bulk and boundary in non-Hermitian quantum walks have also been established [48]. In [49], the authors have introduced the non-hermiticity by making partial measurements on the internal states of the walker and showed the robustness of the topological phases against the disorder. The same model was extended to study higher winding numbers [50]. We use a different model to introduce non-Hermiticity and establish the *persistent* nature of topological phases in these systems. We show that the topological nature of the underlying Hamiltonian does not change in the noisy environment within certain limits. In the case of a 2D quantum walk, another interesting point is the noise-induced topological phase transition, which is absent in the 1D case.

The article is organized as follows: In Sec. II, we discuss the topics which are relevant for the understanding of our results. Sec. III contains our results on the effect

* dey@iisermohali.ac.in

† skgoyal@iisermohali.ac.in

of the losses on the topological nature of quantum walks. Here, we discuss the 1D SSQW and 2D quantum walks and show the persistence of topological phases in noisy environment. We conclude in Sec. IV.

II. BACKGROUND

In this section, we introduce the topics which are relevant to understand our results. We start with 1D and 2D unitary as well as non-unitary DTQWs. Specifically, we discuss the 1D DTQW, 1D SSQW and 2D DTQW and the topological classes arising in these systems. Methods to characterize the topological phases are also discussed in this section.

A. 1D DTQW

DTQW of a quantum walker over a one-dimensional lattice consists of a conditional shift operator T and a coin flip operator $R(\theta)$ for a real parameter θ . In position basis $\{|n\rangle\} \in \mathcal{H}_{\text{pos}}$ and spin basis $\{|\uparrow\rangle, |\downarrow\rangle\}$, the operator $U(\theta) = TR(\theta)$ governs the time evolution of the walker for a unit time on the lattice. Here

$$T = \sum_n |\uparrow\rangle \langle \uparrow| \otimes |n+1\rangle \langle n| + |\downarrow\rangle \langle \downarrow| \otimes |n-1\rangle \langle n|, \quad (1)$$

$$R(\theta) = e^{-i\theta\sigma_y/2} \otimes \mathbb{1}, \quad (2)$$

and $-2\pi \leq \theta < 2\pi$ is a real parameter and σ_y is the Pauli matrix along y -axis. Here, $\mathbb{1}$ represents the identity operation on the lattice. The operator $U(\theta)$ can be expressed in terms of the underlying Hamiltonian $H(\theta)$ as $U(\theta) = e^{-iH(\theta)}$ [22]. For simplicity, we have assumed $\hbar = 1$ and the periodic boundary condition with N number of lattice sites. Since the unitary operator $U(\theta)$ and the Hamiltonian are translation invariant, the (quasi) momentum eigenbasis $\{|k\rangle\}$ are also the energy eigenstates. These states are defined as

$$|n\rangle = \frac{1}{\sqrt{N}} \sum_k \omega^{kn} |k\rangle, \quad \omega = e^{i2\pi/N},$$

with $-N/2 \leq k \leq N/2$ being the quasi-momentum. The Hamiltonian $H(\theta)$ in the quasi-momentum space reads [22]

$$H(\theta) = \sum_k [E_\theta(k) \mathbf{n}_\theta(k) \cdot \boldsymbol{\sigma}] \otimes |k\rangle \langle k|, \quad (3)$$

where the energy $E_\theta(k)$ and the unit Bloch vector $\mathbf{n}_\theta(k)$ read $\cos E_\theta(k) = \cos(\theta/2) \cos k$, and

$$\mathbf{n}_\theta(k) = \frac{(\sin(\theta/2) \sin k, \sin(\theta/2) \cos k, -\cos(\theta/2) \sin k)}{\sin E_\theta(k)} \quad (4)$$

B. 1D SSQW

A more enriched class of 1D DTQW is SSQW, which involves splitting the conditional shift operator T into left-shift (T_\downarrow) and right-shift (T_\uparrow) operators, separated by an additional coin toss $R(\theta_2)$ [22]. The resultant time evolution operator for split-step quantum walks (in one-dimension) reads

$$U_{\text{ss}}(\theta_1, \theta_2) = T_\downarrow R(\theta_2) T_\uparrow R(\theta_1), \quad (5)$$

where

$$T_\downarrow = \sum |\uparrow\rangle \langle \uparrow| \otimes \mathbb{1} + |\downarrow\rangle \langle \downarrow| \otimes |n-1\rangle \langle n|, \\ T_\uparrow = \sum |\uparrow\rangle \langle \uparrow| \otimes |n+1\rangle \langle n| + |\downarrow\rangle \langle \downarrow| \otimes \mathbb{1}.$$

In this case, the effective Hamiltonian $H_{\text{ss}}(\theta_1, \theta_2)$ can be written down in quasi-momentum space as

$$H_{\text{ss}}(\theta_1, \theta_2) = \sum_k [E_{\theta_1, \theta_2}(k) \mathbf{n}_{\theta_1, \theta_2}(k) \cdot \boldsymbol{\sigma}] \otimes |k\rangle \langle k|. \quad (6)$$

The energy and the components of the Bloch vector are given by

$$\cos E_{\theta_1, \theta_2}(k) = \cos(\theta_1/2) \cos(\theta_2/2) \cos k \\ - \sin(\theta_1/2) \sin(\theta_2/2), \quad (7)$$

and $\mathbf{n}_{\theta_1, \theta_2}(k) = n_x(k) \hat{\mathbf{i}} + n_y(k) \hat{\mathbf{j}} + n_z(k) \hat{\mathbf{k}}$ with

$$n_x(k) = \frac{\sin(\theta_1/2) \cos(\theta_2/2) \sin k}{\sin E_{\theta_1, \theta_2}(k)}, \\ n_y(k) = \frac{\cos(\theta_1/2) \sin(\theta_2/2) + \sin(\theta_1/2) \cos(\theta_2/2) \cos k}{\sin E_{\theta_1, \theta_2}(k)}, \\ n_z(k) = \frac{-\cos(\theta_1/2) \cos(\theta_2/2) \sin k}{\sin E_{\theta_1, \theta_2}(k)}. \quad (8)$$

Even though 1D SSQW seems complicated when it comes to implementation, it is not much different from ordinary 1D DTQW; 1D SSQW can be decomposed in two steps of ordinary 1D DTQW [46]. If we consider the SSQW only on the even lattice sites, i.e., instead of hopping on neighboring lattice sites, if the walker hops on next nearest neighbors then the 1D SSQW is equivalent to a quantum walker performing ordinary 1D DTQW, with alternate coin operations on each step. Therefore, the 1D SSQW time evolution operator can be written as

$$U_{\text{ss}}(\theta_1, \theta_2) = U(\theta_2) U(\theta_1). \quad (9)$$

C. 2D DTQW

There are several ways of defining a 2D DTQW in a lattice. For our purpose we introduce the one in which we have a square lattice and a two-dimensional coin [22]. This DTQW consists of two conditional translations in

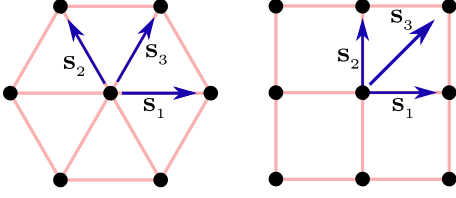


FIG. 1. (Color online) 2D DTQW with nontrivial topology on a triangular lattice and its equivalent square lattice.

two directions accompanied by rotation of the coin. The time evolution operator of 2D DTQW can be written as

$$U_{2D}(\theta_1, \theta_2) = T_y R(\theta_2) T_x R(\theta_1), \quad (10)$$

where T_x and T_y are the translation operators, which translate the particle in x and y directions, respectively. We can also define, 2D DTQW on a triangular lattice which consists of three spin dependent translations separated by coin-slip operations. In that case, the unitary operator which governs the time evolution is written as

$$\tilde{U}_{2D}(\theta_1, \theta_2) = T_{xy} R(\theta_1) T_y R(\theta_2) T_x R(\theta_1), \quad (11)$$

where $T_i (i = x, y, xy)$ are the translations along \mathbf{s}_i directions with $T_{xy} = T_x T_y$, as shown in the Fig. 1. We can derive another two-dimensional quantum walk which is unitarily equivalent to $\tilde{U}_{2D}(\theta_1, \theta_2)$ as $\tilde{U}_{2D} \rightarrow U_{2D} = T_x^\dagger \tilde{U}_{2D} T_x$. The resulting time evolution unitary operator can be written as

$$U_{2D}(\theta_1, \theta_2) = T_y R(\theta_1) T_y R(\theta_2) T_x R(\theta_1) T_x. \quad (12)$$

The underlying Hamiltonian for this quantum walk (in quasi-momentum space) reads

$$H_{2D}(\theta_1, \theta_2) = \sum_{k_x, k_y} E(k_x, k_y) \hat{\mathbf{n}}(k_x, k_y) \cdot \boldsymbol{\sigma} \otimes |k_x, k_y\rangle \langle k_x, k_y|, \quad (13)$$

where the expression of quasi-energy reads

$$\begin{aligned} \cos E(k_x, k_y) &= \cos \theta_1 \cos(\theta_2/2) \cos^2(k_x + k_y) \\ &\quad - \sin \theta_1 \sin(\theta_2/2) \cos(k_x + k_y) \cos(k_x - k_y) \\ &\quad - \cos(\theta_2/2) \sin^2(k_x + k_y), \end{aligned} \quad (14)$$

and the Bloch vector reads [22]

$$\hat{\mathbf{n}}(k_x, k_y) = \frac{n_x(k_x, k_y) \hat{\mathbf{i}} + n_y(k_x, k_y) \hat{\mathbf{j}} + n_z(k_x, k_y) \hat{\mathbf{k}}}{\sin E(k_x, k_y)}, \quad (15)$$

with

$$\begin{aligned} n_x(k_x, k_y) &= -\sin \theta_1 \cos(\theta_2/2) \cos(k_x + k_y) \sin(k_x - k_y) \\ &\quad - \cos^2 \theta_1 \sin(\theta_2/2) \sin 2(k_x - k_y), \\ n_y(k_x, k_y) &= \sin \theta_1 \cos(\theta_2/2) \cos(k_x + k_y) \cos(k_x - k_y) \\ &\quad + \cos \theta_1 \cos^2(k_x - k_y) \sin(\theta_2/2) \\ &\quad - \sin^2(k_x - k_y) \sin(\theta_2/2), \\ n_z(k_x, k_y) &= -\cos^2(\theta_1/2) \cos(\theta_2/2) \sin 2(k_x + k_y) \\ &\quad + \sin \theta_1 \sin(\theta_2/2) \sin(k_x + k_y) \cos(k_x - k_y). \end{aligned} \quad (16)$$

The purpose of writing the evolution for 2D DTQW as (12) is that now it can be decomposed as two 1D SSQW in two different directions, i.e., [46]

$$U_{2D}(\theta_1, \theta_2) = U_{ss}^y(\theta_1, 0) U_{ss}^x(\theta_1, \theta_2), \quad (17)$$

where U_{ss}^i is the time-evolution operator of 1D SSQW (5).

D. Characterizing Topological Phases

Topological phase or topological order is defined as the ground state degeneracy in a quantum system due to the topological properties of the parameter space. The topological nature of these phases make them robust against local perturbations. Topologically ordered states (topological phases) possess non-Abelian geometric phases which are quantized. Tuning the parameters of the Hamiltonian may result in the system going from one topological phase to another as a result of topological phase transition, without breaking the underlying symmetry of the Hamiltonian.

Topological phases can be characterized and classified into various classes using different parameters. In 1D systems, winding number is the topological invariant that characterizes the topological phase. For a given Hamiltonian $H = \bigoplus_k H(k)$, the winding number W_m for the m th band is defined as

$$W_m = \frac{1}{\pi} \int_{\Gamma} \mathcal{A}_m(k) dk, \quad (18)$$

where \mathcal{A}_m is the Berry connection given as [51]

$$\mathcal{A}_m(k) = -i \langle \psi_m(k) | \frac{\partial}{\partial k} | \psi_m(k) \rangle. \quad (19)$$

Here, $|\psi_m(k)\rangle$ is the m th eigenstate of $H(k)$ for the parametric value k . Geometrically, the winding number W_m represents the number of times the Bloch vector \mathbf{n} corresponding to the state $|\psi_m(k)\rangle$ goes around the origin in the counter-clockwise direction as k runs over the first Brillouin Zone. In two or higher dimensional systems, Chern number [52] is one of the topological invariant which is used and defined as

$$C_m = \frac{1}{2\pi} \oint_S \mathcal{F}_m d^2 \mathbf{k}, \quad (20)$$

for $\mathcal{F}_m = \nabla \times \mathcal{A}_m$ and the integration is over the closed surface in two-dimensions (two-dimensional Brillouin zone). Here, \mathcal{A} is the Berry curvature.

Quantum walk Hamiltonian possesses rich topological structure. For example, the Hamiltonian $H_{ss}(\theta_1, \theta_2)$ (6) corresponding to 1D SSQW with parameters θ_1 and θ_2 exhibits two different topological phases characterized by the winding number $W = 0$ and $W = 1$, as shown in Fig. 2(a). In Fig. 2(b), we plot the topological phases with Chern number $C = 0, \pm 1$ exhibited by the Hamiltonian H_{2D} (13) for 2D DTQW.

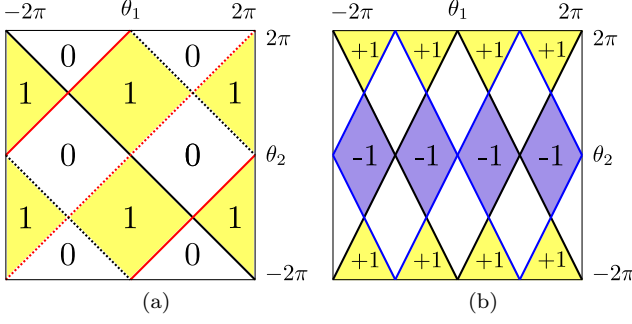


FIG. 2. (Color online) (a) Different topological phases realized in 1D SSQW as a function of θ_1 and θ_2 . Here, black and red lines represent closing of energy band at $k = 0$ and $k = \pi$, respectively, and solid and dotted lines demonstrate the closing at $E = 0$ and $E = \pi$, respectively. (b) Topological phases which exist in 2D DTQW for different values of θ_1 and θ_2 . Here, blue and black lines show the closing of energy gap at $E = 0$ and $E = \pi$, respectively. The yellow, violet and white regions correspond to $C = +1, -1$ and 0 , respectively.

E. Non-unitary Quantum Walk

Quantum walk dynamics is inherently unitary, hence, unlike classical random walks there is no randomness in the quantum walks. However, limitations in physical implementation and the environmental effects can cause losses which can cause the dynamics to deviate from unitary nature.

In general, one can extend 1D SSQW to non-unitary quantum walk by introducing a scaling operator G [43], with tunable parameters in the dynamics. The resulting time evolution operator for non-unitary quantum walk can be written as

$$U_{\text{ss}}^{\text{NU}} = T_{\downarrow} G_2 R(\theta_2) T_{\uparrow} G_1 R(\theta_1), \quad (21)$$

with

$$G_i = \sum_n \begin{pmatrix} g_{i,\uparrow}(n) & 0 \\ 0 & g_{i,\downarrow}(n) \end{pmatrix} \otimes |n\rangle\langle n|. \quad (22)$$

If $g_{i,\uparrow}, g_{i,\downarrow} \neq 1$ then G_i as well as U become nonunitary. For simplicity, we consider the case of homogeneous quantum walk, where all the $g_i(n)$ are independent of n and the scaling operator is written as

$$G_2 = G_1^{-1} = G_{\delta} = \begin{pmatrix} e^{\delta} & 0 \\ 0 & e^{-\delta} \end{pmatrix} \otimes \mathbb{1}. \quad (23)$$

The above choice of operators is motivated by the experimental setup used in [34]. The factor δ is known as the loss and gain factor as the operator G results in increasing (decreasing) the amplitude of spin-up (down). The time evolution operator for non-unitary quantum walk becomes

$$U_{\text{ss}}^{\text{NU}} = T_{\downarrow} G_{\delta} R(\theta_2) T_{\uparrow} G_{\delta}^{-1} R(\theta_1). \quad (24)$$

This particular choice of the scaling operator leaves the translational symmetry of the quantum walk intact. Hence, the dynamical operator can be block-diagonalized in the momentum basis as

$$U_{\text{ss}}^{\text{NU}} = \sum_k \tilde{U}_{\text{ss}}^{\text{NU}}(k) \otimes |k\rangle\langle k|, \quad (25)$$

where

$$\tilde{U}_{\text{ss}}^{\text{NU}}(k) = T_{\downarrow}(k) G_{\delta} R(\theta_2) T_{\uparrow}(k) G_{\delta}^{-1} R(\theta_1), \quad (26)$$

with $T_{\downarrow}(k) = e^{ik(\sigma_z + \mathbb{1})/2}$, $T_{\uparrow}(k) = e^{ik(\sigma_z - \mathbb{1})/2}$ and it acts only on the coin part. The corresponding generator or an effective Hamiltonian $H_{\text{NU}}(\theta_1, \theta_2, \delta)$ reads

$$H_{\text{NU}}(\theta_1, \theta_2, \delta) = \bigoplus_k E(k) \hat{\mathbf{n}}(k) \cdot \boldsymbol{\sigma}, \quad (27)$$

with quasi-energy

$$\cos E(k) = \cos \frac{\theta_1}{2} \cos \frac{\theta_2}{2} \cos k - \sin \frac{\theta_1}{2} \sin \frac{\theta_2}{2} \cosh 2\delta, \quad (28)$$

and $\hat{\mathbf{n}} = n_x(k)\hat{\mathbf{i}} + n_y(k)\hat{\mathbf{j}} + n_z(k)\hat{\mathbf{k}}$ with

$$\begin{aligned} n_x(k) &= \frac{\sin \frac{\theta_1}{2} \cos \frac{\theta_2}{2} \sin k - i \cos \frac{\theta_1}{2} \sin \frac{\theta_2}{2} \sinh 2\delta}{\sin E(k)}, \\ n_y(k) &= \frac{\sin \frac{\theta_1}{2} \cos \frac{\theta_2}{2} \cos k + \cos \frac{\theta_1}{2} \sin \frac{\theta_2}{2} \cosh 2\delta}{\sin E(k)}, \\ n_z(k) &= \frac{-\cos \frac{\theta_1}{2} \cos \frac{\theta_2}{2} \sin k - i \sin \frac{\theta_1}{2} \sin \frac{\theta_2}{2} \sinh 2\delta}{\sin E(k)}. \end{aligned} \quad (29)$$

Note that, for $\delta \neq 1$, G and U are no longer unitary operators and the norm of the state in the evolution may not be preserved. Consequently, $H_{\text{NU}}(\theta_1, \theta_2, \delta)$ is not Hermitian but still we have a real spectrum up to a certain critical value of δ which is given by

$$\delta_c = \frac{1}{2} \cosh^{-1} \left[\frac{\cos \theta_1/2 \cos \theta_2/2 \cos k - \cos E}{\sin \theta_1/2 \sin \theta_2/2} \right], \quad (30)$$

for which the band gap closes. Note, that the argument of \cosh^{-1} in above equation becomes negative when θ_1 and θ_2 have the same sign which results in complex δ_c . So we consider a complex δ given by

$$\delta = \gamma + i\phi. \quad (31)$$

We observe that the negative argument of \cosh^{-1} results in $\phi_c = \pi/2$. We restrict ourselves to the case when δ_c is real and refer γ as the scaling factor. The point γ_c , given by

$$\gamma_c = \frac{1}{2} \cosh^{-1} \left[\frac{\cos \theta_1/2 \cos \theta_2/2 \cos k - \cos E}{\sin \theta_1/2 \sin \theta_2/2} \right] \quad (32)$$

is the point where the \mathcal{PT} -symmetry of the system breaks spontaneously (also known as the exceptional point [53]), and we will have complex energies for $\gamma > \gamma_c$.

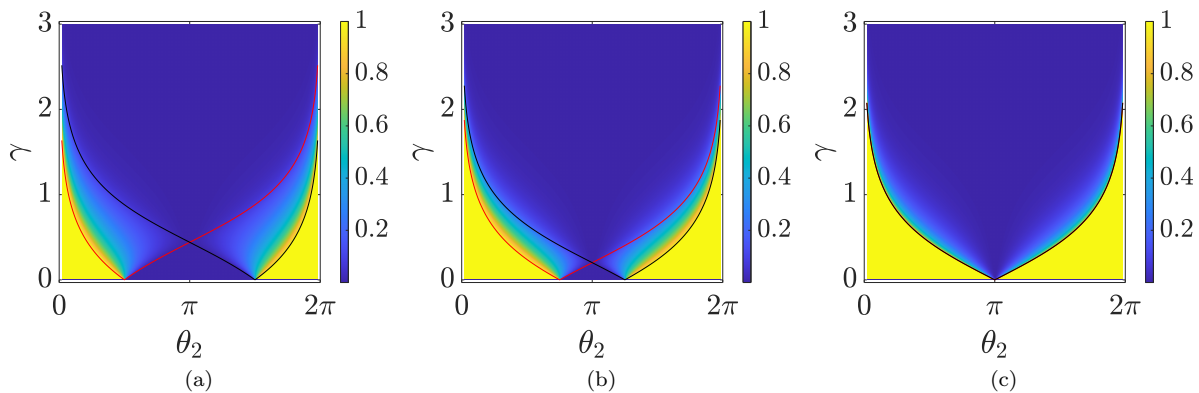


FIG. 3. (Color online) Winding number for lower energy band W_- as a function of γ and θ_2 , and (a) $\theta_1 = -\pi/2$ (b) $\theta_1 = -3\pi/4$ (c) $\theta_1 = -\pi$. The system size is taken to be $N = 100$. The red and black lines in all of the panels represent γ_c for $(k, E) = (0, 0)$ and $(k, E) = (\pi, 0)$, respectively.

III. RESULTS

In this section, we study the behavior of the topological phases in 1D SSQW and 2D DTQW by introducing a nonzero scaling factor γ which, essentially, makes the system non-Hermitian. In 1D SSQW, we find that the topological phases are unaffected even when the system is non-Hermitian (i.e., $\gamma \neq 0$), as far as the system possesses a real spectrum following the \mathcal{PT} -symmetry. However, the topological nature of the system vanishes asymptotically as we cross the exceptional point γ_c , which means the winding number W decays asymptotically for $\gamma > \gamma_c$. We observe the persistence of the Chern number C in 2D DTQW as well until the scaling factor γ reaches a critical value. However, unlike the 1D case, we cannot associate any symmetry breaking with the point where the topological phase transition happens due to the absence of the symmetry in 2D DTQW. Furthermore, we observe the noise induced topological phase transition.

A. Topological phases in 1D non-unitary quantum walk

We start our analysis with non-unitary 1D SSQW, with the associated non-Hermitian Hamiltonian $H_{\text{NU}}(\theta_1, \theta_2, \gamma)$ being given by (27). Since, the Hamiltonian is traceless for all values of γ , the corresponding eigenvalues will always be of the form of $\pm E(k)$. For each momentum k , we compute the energy eigenstates $|\psi_{\pm}(k)\rangle$ corresponding to energies $\pm E(k)$ and, we call the set $\{|\psi_{-}(k)\rangle\}$ and $\{|\psi_{+}(k)\rangle\}$ as the lower and upper energy bands, respectively. Using the expression for the winding number W from (18), we calculate the winding numbers for the lower and upper bands and we name them as W_- and W_+ , respectively.

Since, the eigenstates and eigenvalues depend on γ , θ_1 and θ_2 , the winding numbers are also expected to depend upon these parameter. In Fig. 3, we plot the winding

number for the lower band W_- as a function of γ and θ_2 for different values of θ_1 . In all figures, we notice that for $\gamma = 0$, the winding number can take two different values, zero and one, depending on the choice of θ_1 and θ_2 . Focusing on the case of $W_- = 1$ for a vanishing γ , we observe that for a given (θ_1, θ_2) if we increase the value of γ , the winding number remains unaffected until we approach the critical value of γ , i.e., γ_c (32). Crossing the γ_c causes a phase transition and the value of the winding number starts decreasing and approaches zero asymptotically. Whereas, if initially the winding number $W_- = 0$, it remains zero until we approach γ_c , and then it starts to increase momentarily approaching some maximum value and then deteriorates to zero asymptotically.

By definition, the winding number is an integer quantity. In other words, the geometric phase acquired by the eigenstates of the Hamiltonian in the k -space is quantized and is a multiple of π , which is possible only when all the states in an energy band lie on a geodesic in the Bloch sphere. The winding number must always be an integer for all the Hermitian Hamiltonians. However, as a matter of fact, W can take non-integer values for 1D SSQW in \mathcal{PT} -symmetry broken region. This can be explained by observing the behaviour of the eigenstates of the non-Hermitian Hamiltonian. In Fig. 4, we plot the Bloch vectors corresponding to the eigenstates $|\psi(k)\rangle$ of the Hamiltonian $H_{\text{NU}}(\theta_1, \theta_2, \gamma)$ on the Bloch sphere. Figs. 4(a) and 4(b) are for $\gamma \leq \gamma_c$ whereas Figs. 4(c) and 4(d) are for $\gamma > \gamma_c$. We can clearly see that in the unbroken \mathcal{PT} -symmetric region, the eigenstates lie in a plane and results in integer value of the winding number, whereas in the \mathcal{PT} -symmetry broken region the eigenvectors trace a path which does not lie on a great circle. Hence geometric phase is not a multiple of π .

In summary, we have shown that the topological phase in 1D SSQW remains invariant as long as the energy eigenvalues are real, even though the Hamiltonian is not Hermitian, i.e., the topological order persists as long as the Hamiltonians are \mathcal{PT} symmetric. Next we extend

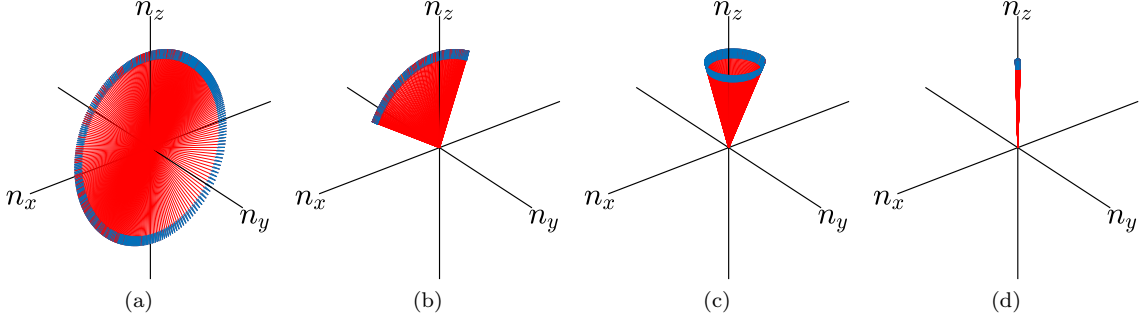


FIG. 4. (Color online) Winding of the Bloch vector around the origin with the lattice size, $N = 100$ (a) $\theta_1 = -3\pi/8$, $\theta_2 = \pi/8$, $\gamma = 0.25$ (b) $\theta_1 = -3\pi/8$, $\theta_2 = 5\pi/8$, $\gamma = 0.25$ (c) $\theta_1 = -3\pi/8$, $\theta_2 = \pi/8$, $\gamma = 1.8$ (d) $\theta_1 = -3\pi/8$, $\theta_2 = \pi/8$, $\gamma = 3.0$.

our study to the case of 2D DTQW.

B. Topological phases in 2D non-unitary quantum walk

Since, 2D DTQW can be decomposed as a product of two 1D SSQW, we can easily extend 2D DTQW to non-unitary limits by introducing the scaling operator G along one axis only (say x -axis). The time evolution operator can be written as

$$U_{2D}^{\text{NU}}(\theta_1, \theta_2, \gamma) = T_y R(\theta_1) T_y R(\theta_2) G_\gamma T_x R(\theta_1) G_\gamma^{-1} T_x. \quad (33)$$

The corresponding non-Hermitian Hamiltonian of this system reads

$$H_{2D}^{\text{NU}}(\theta_1, \theta_2, \gamma) = \bigoplus_{k_x, k_y} E(k_x, k_y, \gamma) \mathbf{n}(k_x, k_y, \gamma) \cdot \boldsymbol{\sigma}, \quad (34)$$

where

$$\begin{aligned} \cos E(k_x, k_y, \gamma) &= \cos \theta_1 \cos \theta_2 / 2 \cos(k_x + k_y - i\gamma) \cos(k_x + k_y + i\gamma) \\ &\quad - \cos \theta_2 / 2 \sin(k_x + k_y - i\gamma) \sin(k_x + k_y + i\gamma) \\ &\quad - \sin \theta_1 \sin \theta_2 / 2 \cos(k_x - k_y - i\gamma) \cos(k_x + k_y + i\gamma), \end{aligned} \quad (35)$$

and

$$\hat{\mathbf{n}}(k_x, k_y) = \frac{n_x(k_x, k_y) \hat{\mathbf{i}} + n_y(k_x, k_y) \hat{\mathbf{j}} + n_z(k_x, k_y) \hat{\mathbf{k}}}{\sin E(k_x, k_y)}, \quad (36)$$

with

$$\begin{aligned} n_x(k_x, k_y) &= \\ &\quad - \sin \theta_1 \cos(\theta_2/2) \cos(k_x + k_y - i\gamma) \sin(k_x - k_y + i\gamma) \\ &\quad - \cos \theta_1 \sin(\theta_2/2) \cos(k_x - k_y - i\gamma) \sin(k_x - k_y + i\gamma) \\ &\quad - \sin(\theta_2/2) \sin(k_x - k_y - i\gamma) \cos(k_x - k_y + i\gamma), \\ n_y(k_x, k_y) &= \\ &\quad \sin \theta_1 \cos(\theta_2/2) \cos(k_x + k_y - i\gamma) \cos(k_x - k_y + i\gamma) \\ &\quad + \cos \theta_1 \sin(\theta_2/2) \cos(k_x - k_y - i\gamma) \cos(k_x - k_y + i\gamma) \\ &\quad - \sin(\theta_2/2) \sin(k_x - k_y - i\gamma) \sin(k_x - k_y + i\gamma), \\ n_z(k_x, k_y) &= \\ &\quad - \cos \theta_1 \cos(\theta_2/2) \cos(k_x + k_y - i\gamma) \sin(k_x + k_y + i\gamma) \\ &\quad - \cos(\theta_2/2) \sin(k_x + k_y - i\gamma) \cos(k_x + k_y + i\gamma) \\ &\quad + \sin \theta_1 \sin(\theta_2/2) \cos(k_x - k_y - i\gamma) \sin(k_x + k_y + i\gamma). \end{aligned}$$

The 2D DTQW is different from the 1D SSQW as in the former case, energy eigenvalues become complex even for a very small values of γ . Therefore, 2D DTQW does not support \mathcal{PT} -symmetry even for very small values of scaling factor. For $\gamma \ll 1$ the expression for the energy reads

$$\cos E(\gamma) = \cos E(\gamma = 0) + i\gamma \sin \theta_1 \sin \theta_2 / 2 \sin(2k_y) \quad (37)$$

which makes the quasi-energy complex for infinitesimal scaling parameter γ . It shows the absence of \mathcal{PT} -symmetry in 2D DTQW.

Similar to the case of 1D SSQW, in 2D quantum walks also the energy eigenvalues appear in pairs $\pm E(k_x, k_y, \gamma)$ resulting in two energy bands. Introducing loss and gain (scaling factor γ) in x -direction results in complex pairs of energy eigenvalues. We can choose the lower energy state by looking at the sign of the real part of the energy eigenstate and calculate the Chern number.

We use (20) to calculate the Chern number for the lower energy band and plot it against γ and θ_2 for some fixed values of θ_1 (Fig. 5). Despite the absence of \mathcal{PT} -symmetry, we see the persistence of the topological phase as we turn on the scaling $\gamma \neq 0$. In other words, the system remains in the same topological phase as we introduce loss and gain factors. In 2D DTQW we observe an-

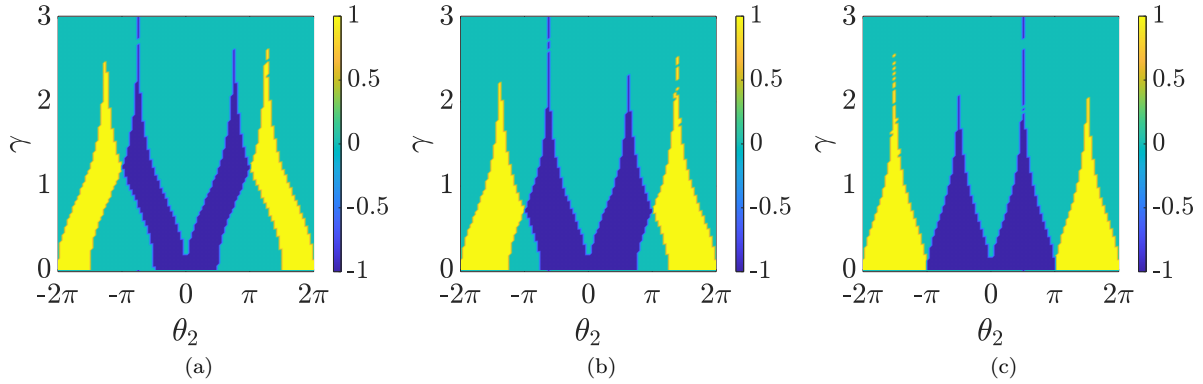


FIG. 5. (Color online) Effect of γ on Chern number is plotted with varying θ_2 for (a) $\theta_1 = \pi/4$ (b) $\theta_1 = 3\pi/8$ (c) $\theta_1 = 3\pi/2$. The system size is taken to be 50.

other interesting feature, namely, for some particular values of θ_1 and θ_2 , the Chern number can change abruptly from one integer value to another, resulting to a non-trivial topological phase transition. This is a noise induced topological phase transition. Furthermore, unlike the 1D SSQW the Chern number in 2D DTQW changes abruptly and for sufficiently large values of γ the Chern number for all the parameters becomes zero.

IV. CONCLUSION

We have studied the effect of a lossy environment on the topological properties of discrete-time quantum walks. Specifically, we have studied the 1D SSQW and 2D DTQW and observed the persistence of topological phases against noise in these systems. The noise is incorporated using the non-Hermitian Hamiltonian approach, where we include a scaling parameter γ which characterizes the non-Hermiticity. We find a strong correspondence between the spontaneous \mathcal{PT} -symmetry breaking and the loss of topological order in 1D SSQW, i.e., the

system retains its topological order for any value of γ , as long as the system is \mathcal{PT} -symmetric. Due to the absence of \mathcal{PT} -symmetry in 2D DTQW upon introducing the noise, we do not observe such correspondence in these systems. However, we observe noise-induced topological phase transition where we see that increasing the scaling parameter γ may transfer the system from one non-trivial topological phase to another. Our results confirm the robustness of the topological properties of DTQWs and the role of noise in a topological phase transition.

ACKNOWLEDGMENTS

S. K. G. acknowledges the financial support from SERB-DST (File No. ECR/2017/002404). S. D. acknowledges the support of research grant (DST/INSPIRE/04/2016/001391) from DST-INSPIRE, Govt. of India. V. M. thanks International Centre for Theoretical Sciences (ICTS) for the hospitality during the program- Geometric phase in Optics and Topological Matter (Code: ICTS/geomtop2020/01).

-
- [1] Y. Aharonov, L. Davidovich, and N. Zagury, Phys. Rev. A **48**, 1687 (1993).
 - [2] A. Ambainis, E. Bach, A. Nayak, A. Vishwanath, and J. Watrous, in *Proceedings of the Thirty-Third Annual ACM Symposium on Theory of Computing*, STOC 01 (Association for Computing Machinery, New York, NY, USA, 2001) pp. 37 – 49.
 - [3] J. Kempe, Contemporary Physics **44**, 307 (2003).
 - [4] S. E. Venegas-Andraca, Quantum Information Processing **11**, 1015 (2012).
 - [5] A. Nayak and A. Vishwanath, arXiv e-prints, quant-ph/0010117 (2000).
 - [6] A. M. Childs, Phys. Rev. Lett. **102**, 180501 (2009).
 - [7] A. M. Childs, D. Gosset, and Z. Webb, Science **339**, 791 (2013).
 - [8] N. B. Lovett, S. Cooper, M. Everitt, M. Trevers, and V. Kendon, Phys. Rev. A **81**, 042330 (2010).
 - [9] A. Ambainis, International Journal of Quantum Information **01**, 507 (2003).
 - [10] A. M. Childs and J. Goldstone, Phys. Rev. A **70**, 022314 (2004).
 - [11] N. Shenvi, J. Kempe, and K. B. Whaley, Phys. Rev. A **67**, 052307 (2003).
 - [12] E. Agliari, A. Blumen, and O. Mülken, Phys. Rev. A **82**, 012305 (2010).
 - [13] F. De Nicola, L. Sansoni, A. Crespi, R. Ramponi, R. Osellame, V. Giovannetti, R. Fazio, P. Mataloni, and F. Sciarrino, Phys. Rev. A **89**, 032322 (2014).
 - [14] P. Kurzyński and A. Wójcik, Phys. Rev. A **83**, 062315 (2011).

- [15] A. Schreiber, A. Gábris, P. P. Rohde, K. Laiho, M. Štefaniák, V. Potoček, C. Hamilton, I. Jex, and C. Silberhorn, *Science* **336**, 55 (2012).
- [16] L. Sansoni, F. Sciarrino, G. Vallone, P. Mataloni, A. Crespi, R. Ramponi, and R. Osellame, *Phys. Rev. Lett.* **108**, 010502 (2012).
- [17] A. Peruzzo, M. Lobino, J. C. F. Matthews, N. Matsuda, A. Politi, K. Poulios, X.-Q. Zhou, Y. Lahini, N. Ismail, K. Wörhoff, Y. Bromberg, Y. Silberberg, M. G. Thompson, and J. L. O'Brien, *Science* **329**, 1500 (2010).
- [18] M. Mohseni, P. Rebentrost, S. Lloyd, and A. Aspuru-Guzik, *The Journal of Chemical Physics* **129**, 174106 (2008).
- [19] A. Romanelli, R. Siri, G. Abal, A. Auyuanet, and R. Donangelo, *Physica A: Statistical Mechanics and its Applications* **347**, 137 (2005).
- [20] V. Kendon, *Mathematical Structures in Computer Science* **17**, 1169 (2007).
- [21] P. Kurzyński and A. Wójcik, *Phys. Rev. Lett.* **110**, 200404 (2013).
- [22] T. Kitagawa, M. S. Rudner, E. Berg, and E. Demler, *Phys. Rev. A* **82**, 033429 (2010).
- [23] T. Kitagawa, M. A. Broome, A. Fedrizzi, M. S. Rudner, E. Berg, I. Kassal, A. Aspuru-Guzik, E. Demler, and A. G. White, *Nature Communications* **3**, 882 (2012).
- [24] J. K. Asbóth, *Phys. Rev. B* **86**, 195414 (2012).
- [25] J. M. Edge and J. K. Asboth, *Phys. Rev. B* **91**, 104202 (2015).
- [26] J. K. Asbóth and H. Obuse, *Phys. Rev. B* **88**, 121406 (2013).
- [27] J. K. Asbóth, B. Tarasinski, and P. Delplace, *Phys. Rev. B* **90**, 125143 (2014).
- [28] B. C. Travaglione and G. J. Milburn, *Phys. Rev. A* **65**, 032310 (2002).
- [29] H. Schmitz, R. Matjeschk, C. Schneider, J. Glueckert, M. Enderlein, T. Huber, and T. Schaetz, *Phys. Rev. Lett.* **103**, 090504 (2009).
- [30] F. Zähringer, G. Kirchmair, R. Gerritsma, E. Solano, R. Blatt, and C. F. Roos, *Phys. Rev. Lett.* **104**, 100503 (2010).
- [31] M. Karski, L. Förster, J.-M. Choi, A. Steffen, W. Alt, D. Meschede, and A. Widera, *Science* **325**, 174 (2009).
- [32] A. Schreiber, K. N. Cassemiro, V. Potoček, A. Gábris, P. J. Mosley, E. Andersson, I. Jex, and C. Silberhorn, *Phys. Rev. Lett.* **104**, 050502 (2010).
- [33] A. Schreiber, K. N. Cassemiro, V. Potoček, A. Gábris, I. Jex, and C. Silberhorn, *Phys. Rev. Lett.* **106**, 180403 (2011).
- [34] A. Regensburger, C. Bersch, M.-A. Miri, G. Onishchukov, D. N. Christodoulides, and U. Peschel, *Nature* **488**, 167 (2012).
- [35] M. A. Broome, A. Fedrizzi, B. P. Lanyon, I. Kassal, A. Aspuru-Guzik, and A. G. White, *Phys. Rev. Lett.* **104**, 153602 (2010).
- [36] P. Zhang, X.-F. Ren, X.-B. Zou, B.-H. Liu, Y.-F. Huang, and G.-C. Guo, *Phys. Rev. A* **75**, 052310 (2007).
- [37] B. Sephton, A. Dudley, G. Ruffato, F. Romanato, L. Marrucci, M. Padgett, S. Goyal, F. Roux, T. Konrad, and A. Forbes, *PLOS ONE* **14**, 1 (2019).
- [38] J. Du, H. Li, X. Xu, M. Shi, J. Wu, X. Zhou, and R. Han, *Phys. Rev. A* **67**, 042316 (2003).
- [39] C. A. Ryan, M. Laforest, J. C. Boileau, and R. Laflamme, *Phys. Rev. A* **72**, 062317 (2005).
- [40] A. Alberti and S. Wimberger, *Phys. Rev. A* **96**, 023620 (2017).
- [41] C. M. Bender and S. Boettcher, *Phys. Rev. Lett.* **80**, 5243 (1998).
- [42] A. Mostafazadeh, *Journal of Mathematical Physics* **43**, 205 (2002).
- [43] K. Mochizuki, D. Kim, and H. Obuse, *Phys. Rev. A* **93**, 062116 (2016).
- [44] L. Xiao, X. Zhan, Z. Bian, K. Wang, X. Zhang, X. Wang, J. Li, K. Mochizuki, D. Kim, N. Kawakami, *et al.*, *Nature Phys.* **13**, 1117 (2017).
- [45] M. S. Rudner and L. S. Levitov, *Phys. Rev. Lett.* **102**, 065703 (2009).
- [46] W.-W. Zhang, S. K. Goyal, C. Simon, and B. C. Sanders, *Phys. Rev. A* **95**, 052351 (2017).
- [47] Y. Wang, Y.-H. Lu, F. Mei, J. Gao, Z.-M. Li, H. Tang, S.-L. Zhu, S. Jia, and X.-M. Jin, *Phys. Rev. Lett.* **122**, 193903 (2019).
- [48] L. Xiao, T. Deng, K. Wang, G. Zhu, Z. Wang, W. Yi, and P. Xue, *Nature Phys.* **16**, 761 (2020).
- [49] X. Zhan, L. Xiao, Z. Bian, K. Wang, X. Qiu, B. C. Sanders, W. Yi, and P. Xue, *Phys. Rev. Lett.* **119**, 130501 (2017).
- [50] L. Xiao, X. Qiu, K. Wang, Z. Bian, X. Zhan, H. Obuse, B. C. Sanders, W. Yi, and P. Xue, *Phys. Rev. A* **98**, 063847 (2018).
- [51] M. V. Berry, *Proceedings of the Royal Society of London. A. Mathematical and Physical Sciences* **392**, 45 (1984).
- [52] J. Asbóth, L. Oroszlány, and A. Pályi, *A Short Course on Topological Insulators: Band Structure and Edge States in One and Two Dimensions*, Lecture Notes in Physics (Springer International Publishing, 2016).
- [53] S. K. Özdemir, S. Rotter, F. Nori, and L. Yang, *Nature Materials* **18**, 783 (2019).